



# A surface plasmon study of the optical dielectric function of indium

J. R. SAMBLES, A. P. HIBBINS, M. J. JORY

Thin Film Photonics Group, School of Physics, University of Exeter,  
Exeter EX4 4QL, UK

and H. AZIZBEKYAN

Engineering Center of Armenian National Academy of Sciences,  
Ashtarak-2, 378410 Armenia

(Received 24 November 1999)

**Abstract.** The optical dielectric function of indium is measured by optical excitation of surface plasmon polaritons on an indium-coated silica grating for a range of wavelengths in the visible region of the spectrum. By exciting the surface plasmon polariton at the buried indium–grating interface, the indium surface that supports the surface plasmon polariton is kept free from oxidation. Comparison of angle-dependent reflectivities with a grating modelling theory gives both the real and imaginary parts of the dielectric function of indium. These results are compared with free-electron models to obtain an estimate of the plasma frequency and relaxation time.

## 1. Introduction

Metals that have negative real parts to their dielectric response function in the visible are able to support optically excited surface plasmon polaritons (SPPs). The best known, and most commonly utilized, are silver [1–5] and gold [3, 6–8] with which a variety of experimental studies have been undertaken. These two metals have received considerable attention for three primary reasons. Firstly they are considered relatively inert and so are not rapidly contaminated allowing free surfaces to be explored in air. Secondly they are quite readily deposited by vacuum evaporation as thin films, which is advantageous for many studies. Thirdly, they have optical permittivities ( $\epsilon = \epsilon_r + i\epsilon_i$ ) that for silver for the whole visible spectrum, and for gold, above 550 nm, satisfy  $|\epsilon_r| \gg \epsilon_i$  and  $\epsilon_r \ll -1$ . This leads to relatively narrow SPP resonances that may be readily observed optically. Other materials that are more easily oxidized have been studied using SPPs at buried interfaces using prism coupling. These include aluminium [9], magnesium [10] and recently zinc [11]. This last study also employs grating coupling to a buried interface, a technique previously used by Nash and Sambles to characterize silver [5] and copper [12]. Here this optical excitation of SPPs at a buried grating interface is extended to an exploration of the dielectric response function of indium.

There are good reasons for supposing that indium will support surface plasmon resonances since its optical response function, as deduced from Th  ye and Devant's work [13] is such as to satisfy  $\epsilon_r \ll -1$  although  $|\epsilon_r|$  is only just larger than  $\epsilon_i$ . This latter fact suggests rather broad resonances. In addition Kovacs [14] recorded surface plasmon resonances from indium films encapsulated by  $\text{MgF}_2$  layers. He explored 19 nm, 27 nm and 42 nm thick indium layers and obtained data with 540 nm light, which gave results consistent with the permittivity given by Th  ye and Devant ( $\epsilon = -29.011 + 9.773i$ ). Examination of the literature reveals that the values given by Th  ye and Devant, deduced from optical reflectance and transmittance of thin films of indium, are probably the most reliable since they have carefully taken into account the oxide layer which inevitably forms when the films are exposed to air. Other results [15–17], also presented by Th  ye and Devant, for the real,  $n$ , and imaginary,  $k$ , parts of the refractive index of thicker indium are substantially different. For example at 2 eV, while Th  ye and Devant give  $\epsilon = -38.4 + 14.3i$ , Ageev and Shklyarevskii [15] find  $\epsilon = -20.4 + 5.0i$  and Glovashkia *et al.* [16] find  $\epsilon = -27.2 + 9.0i$ . (A further study by El Oker *et al.* [18] on thin films shows disturbing variations of  $\epsilon$  with wavelength, having unreasonably small values of  $|\epsilon_r|$ , and should be discounted.) It is in view of these differences, which may in part be due to the lack of correct treatment of the indium oxidation, but may also be associated with the difference in film character, that we have undertaken this study. It is an exploration of the dielectric response function of indium over the visible spectrum by resonant excitation of the SPP at a buried grating interface (protected from oxidation) of a very thick (500 nm), effectively bulk film.

## 2. Experimental

There are two essential requirements for optically exciting SPPs at a clean indium interface. First the interface needs to be protected from oxidation—it needs to be a buried interface. Secondly there has to be a method for providing sufficient in-plane additional momentum to allow coupling of incident photons to the SPP. Both of these requirements are met by depositing, in vacuum, the indium film on to a silica grating. The periodicity of the grating,  $\lambda_g$ , provides the additional in-plane momentum in integral units of  $N/\lambda_g$  (for the plane of incidence containing the grating vector—perpendicular to the grating grooves) to allow coupling between the incident radiation and the SPP. In addition, the depth of the grating dictates the coupling strength.

A grating of pitch of order 800 nm is fabricated in silica by interferographic exposure of a suitable photoresist on a flat silica substrate, followed by chemical development and atom etching. This produces a high quality grating with a well-defined, uniform, pitch and a profile which is slightly distorted from a pure sinusoid. On this cleaned silica grating was deposited, by thermal evaporation in a vacuum of  $<10^{-4}$  Pa, a layer of 99.99% pure indium, to a thickness of order 500 nm (fully optically opaque). On removal from the vacuum this layer was overcoated with a thin lacquer layer to limit progressive oxidation of the indium.

The excitation of SPPs was recorded as minima in the angle dependent reflectivity of p-polarized (transverse magnetic) light incident in a plane normal to the grating groove direction. To allow access to a wide range of in-plane momenta a  $45^\circ$ ,  $45^\circ$ ,  $90^\circ$  silica prism was attached to the flat face of the silica

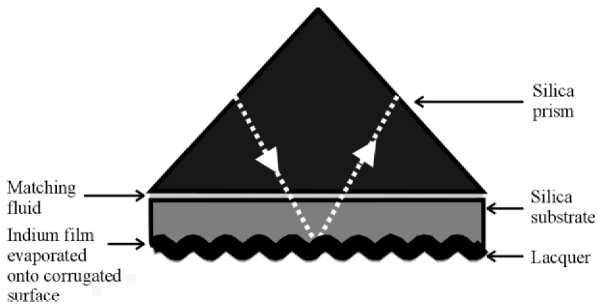


Figure 1. Schematic diagram illustrating the sample used in this study. To allow access to a wide range of in-plane momenta a  $45^\circ$ ,  $45^\circ$ ,  $90^\circ$  silica prism is attached to the flat face of the silica grating substrate by means of a fluid of matching index. Light incident upon the prism passes through the matching fluid and silica substrate and arrives undeflected at the buried silica-indium grating interface. A thin lacquer layer deposited on top of the indium prevents progressive oxidization through the film.

grating substrate by means of a fluid of matching index (figure 1). Light incident upon the prism passes through the matching fluid and silica substrate arriving undeflected at the silica-indium grating interface. Angle-dependent reflectivities were corrected for reflections at the air-prism entrance face and the prism-air exit face, and normalized to the incident beam intensity before being fitted by modelling theory.

Data, which were recorded over the wavelength range 400 to 900 nm, in 25 nm steps were fitted by an iterative least-squares minimization procedure using a scattering matrix [19] program based on a transformed coordinate approach [20]. By use of the most noise-free data taken at the centre of the wavelength range studied it is possible to obtain in detail the grating pitch and the first three Fourier coefficients of its amplitude profile. With this information established, all the remaining data is fitted using these profile parameters to yield  $\epsilon_r$  and  $\epsilon_i$  of the indium layer. Typical fitted data are shown in figure 2.

### 3. Results

The optical permittivity values found from the fits to the angle-dependent reflectivity data are listed in table 1 and presented graphically in figure 3. Also given for comparison are some of the results of Th  ye and Devant over the same region of the spectrum. There are clearly systematic discrepancies between the two sets of data with the real permittivities deduced here being less negative and the imaginary permittivities being less positive. However the data show similar overall trends with  $\epsilon_r$  becoming more negative in an almost linear fashion with wavelength while  $\epsilon_i$  rises more rapidly. The simplest explanation for the differences between the data rests with the form of the sample. The sample used here is much thicker, it is protected from oxidation and will correspondingly have a different grain structure and a different resistivity scattering time.

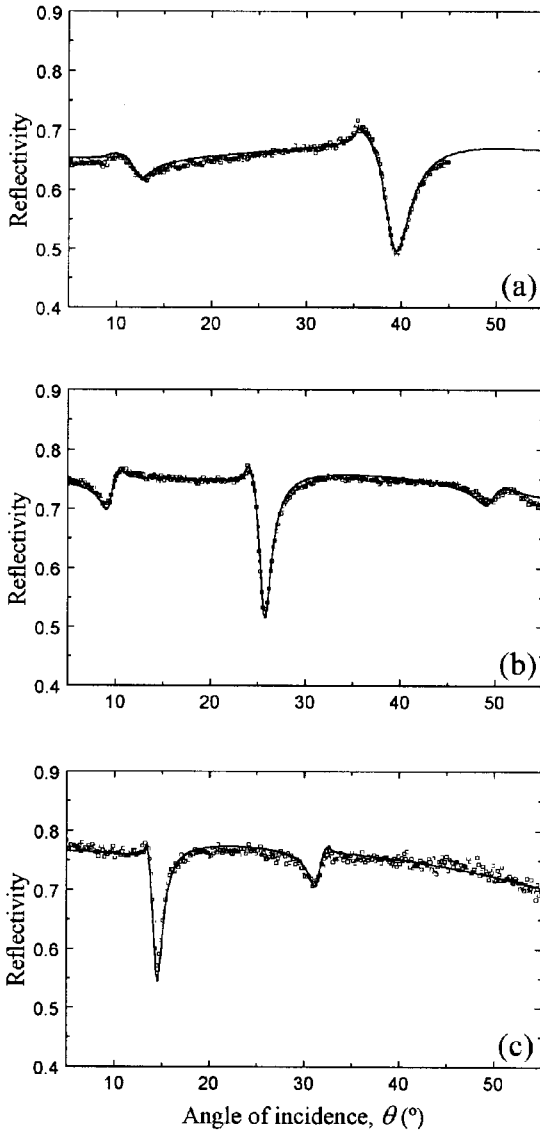


Figure 2. Typical experimental angle-dependent reflectivities ( $\square$ , only one point in five plotted for clarity) compared with the theoretically-modelled reflectivities ( $—$ ) created from a single set of grating profile parameters. (a), (b) and (c) show the  $R_{pp}$  reflectivity measurements (i.e. p-polarized (transverse magnetic) radiation was incident and detected) at incident wavelengths of 500 nm, 700 nm and 900 nm respectively. The value of the dielectric constants that were obtained by fitting the model to the experimental data for each wavelength studied are shown in table 1.

#### 4. Discussion

Because of the simple functional dependence of  $\epsilon_r$  on wavelength seen in figure 3, it is tempting to use a Drude model to interpret the data. From the Drude model we expect

$$\epsilon_r(\omega) = \epsilon(\infty) - \frac{\omega_{pT}^2}{1 + \omega^2\tau^2} \quad (1)$$

Table 1. The optical dielectric function of indium experimentally determined in this work, together with the results determined by Théye and Devant [13].

Wavelength (nm)				Wavelength (nm)			
	$\epsilon_r$	$\epsilon_i$	Reference		$\epsilon_r$	$\epsilon_i$	Reference
400	-15.9	4.3	[13]	600	-26.8	9.4	this work
400	-11.8	3.6	this work	625	-30.0	10.5	this work
420	-17.4	4.9	[13]	650	-39.0	15.7	[13]
425	-13.4	4.1	this work	650	-31.1	11.3	this work
440	-19.1	5.6	[13]	675	-33.2	12.3	this work
450	-15.9	4.8	this work	700	-45.7	18.4	[13]
460	-21.1	6.3	[13]	700	-35.6	13.2	this work
475	-17.6	5.6	this work	725	-36.7	14.3	this work
480	-22.9	7.1	[13]	750	-51.8	22.6	[13]
500	-25.5	8.2	[13]	750	-39.2	15.4	this work
500	-19.6	6.7	this work	775	-41.0	16.9	this work
520	-26.7	8.8	[13]	800	-56.2	26.8	[13]
525	-21.9	7.1	this work	800	-41.7	17.6	this work
540	-28.8	10.0	[13]	825	-43.7	19.4	this work
550	-23.3	7.9	this work	850	-62.8	31.6	[13]
560	-30.4	10.8	[13]	850	-45.3	20.7	this work
575	-24.8	8.3	this work	875	-46.9	21.9	this work
580	-32.5	11.7	[13]	900	-64.6	35.2	[13]
600	-34.0	12.6	[13]	900	-47.5	23.8	this work

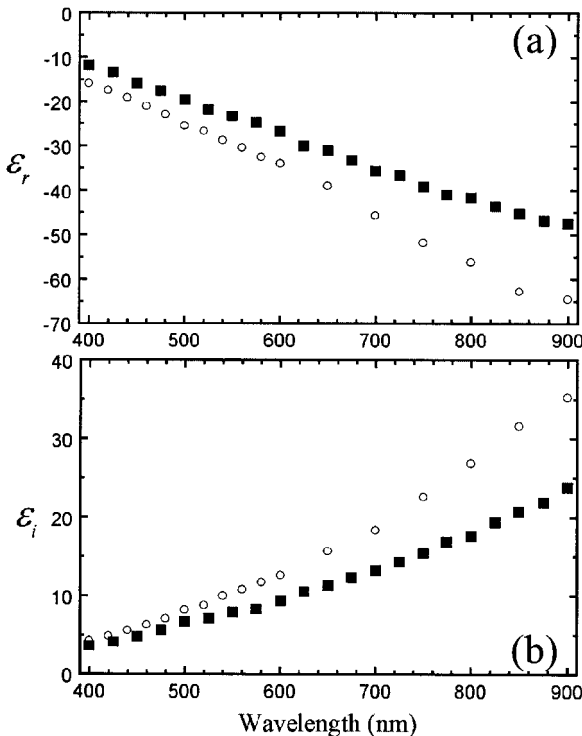


Figure 3. A comparison of the values of the dielectric function of indium determined in this work (■), compared with those determined by Théye and Devant (○). Top: (a) real component ( $\epsilon_r$ ). Bottom: (b) imaginary component ( $\epsilon_i$ ).

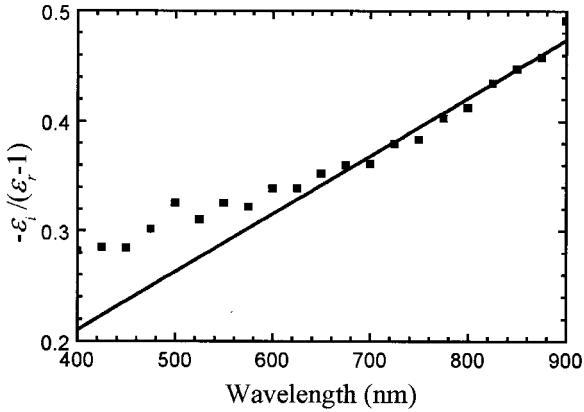


Figure 4. A plot of  $-\varepsilon_i/(\varepsilon_r - 1)$  against  $\lambda_0$  for the values of the dielectric function determined in this work. A high degree of linearity suggests that the indium film is free-electron like. The relaxation time,  $\tau$ , is determined from the gradient of the line of best-fit which also passes through the origin. However, since the sample appears free-electron like at wavelengths in excess of approximately 600 nm, the straight line plotted is a best fit to only the high wavelength data.

and

$$\varepsilon_i(\omega) = \frac{\omega_p^2 \tau}{\omega(1 + \omega^2 \tau^2)}, \quad (2)$$

where  $\varepsilon(\infty)$  is the residual dielectric constant (assumed to be unity),  $\tau$  is the relaxation time of the conduction electrons in indium and  $\omega_p$  is the plasma frequency, which is given by

$$\omega_p^2 = \frac{Ne^2}{\varepsilon(\infty)m^*} \quad (3)$$

where  $N$  is the electron density and  $m^*$  is the effective electron mass. From these free electron expressions for  $\varepsilon_r$  and  $\varepsilon_i$  note that  $-\varepsilon_i/(\varepsilon_r - 1)$  should vary linearly with  $\lambda$ , with a slope of  $1/2\pi c\tau$ . Such a plot is shown in figure 4 giving a straight line from 625 to 900 nm, indicating that indium illustrates free-electron-like behaviour in this range. The gradient from this figure gives a relaxation time of  $(1.01 \pm 0.04) \times 10^{-15}$  s. In addition, figure 5 shows a graph of  $(1 - \varepsilon_r)^{-1}$  plotted against  $\lambda^{-2}$  (an approximation from equation (1)); the gradient of such a plot yields a  $\hbar\omega_p$  value of  $12.8 \pm 1.0$  eV. The errors in all of the above values have been calculated by making a comparison between a straight-line fit to all the data available, and the reduced set of points that form the linear part of the curves. The large error in the value of the plasma frequency is attributable to the strong deviation away from a linear relationship at low wavelengths (figure 5). It is therefore clear that the optical response of indium over the wavelength range studied in this work is not purely Drude-like in nature. In fact, such behaviour is not unexpected since previous workers have shown there to be a number of absorption peaks associated with interband transitions (see e.g. [13, 18]).

Consequently, any accurate representation of the complex dielectric function of indium must involve splitting it into two parts: one part corresponding to the intraband excitations described by the Drude model, and an interband part

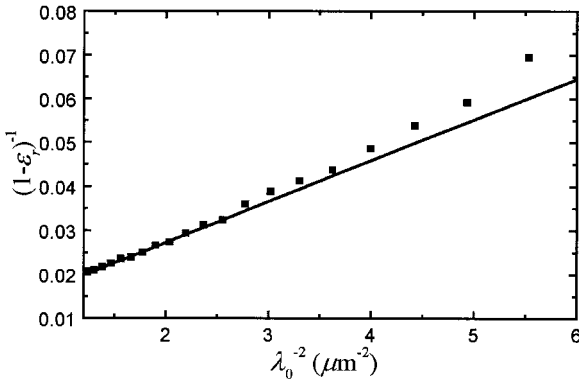


Figure 5. A plot of  $(1 - \epsilon_r)^{-1}$  against  $\lambda_0^{-2}$  for the values of the dielectric function determined in this work. The plasma energy,  $\omega_p$ , is determined from the gradient of the line of best-fit, and using the value of  $\tau$  previously determined. Once again, since the sample appears free-electron like at wavelengths only in excess of approximately 600 nm ( $\lambda_0^{-2} > 2.8 \mu\text{m}^{-2}$ ), the straight line plotted is a best fit to only the high wavelength data.

corresponding to resonant absorptions based on a Lorentz oscillator model. In order to provide a more satisfactory fit to the dielectric function of indium than provided by a simple Drude theory, the experimental data is compared to a model that assumes one absorption peak at frequency  $\omega_0$ . The two parts of the complex dielectric function are therefore

$$\epsilon_r(\omega) = \epsilon(\infty) - \frac{\omega_p^2 \tau^2}{1 + \omega^2 \tau^2} + \frac{\tau^2 \omega_p^2 (\omega_0^2 - \omega^2)}{\tau^2 (\omega_0^2 - \omega^2)^2 + \omega^2} \tag{4}$$

and

$$\epsilon_i(\omega) = \frac{\omega_p^2 \tau}{\omega (1 + \omega^2 \tau^2)} + \frac{\omega_p^2 \omega \tau}{\tau^2 (\omega_0^2 - \omega^2)^2 + \omega^2} \tag{5}$$

By rearranging equations (4) and (5), and setting  $\epsilon(\infty) = 1$ , the following expression is obtained

$$\frac{\epsilon_r(\omega) - 1}{\epsilon_i(\omega)} = \omega \tau \left[ \left( \frac{\omega_0^2 (\omega^2 \tau^2 + 1)}{\omega^2 (\omega^2 \tau^2 + 1) + \tau^2 (\omega_0^2 - \omega^2)^2 + \omega^2} \right) - 1 \right], \tag{6}$$

which is independent of  $\omega_p$ . By fitting the functional form of equation (6) to the experimental data, the constants  $\tau = (1.08 \pm 0.02) \times 10^{-15}$  s and  $\hbar\omega_0 = 6.82 \pm 0.14$  eV are obtained (figure 6). The experimentally determined complex dielectric function may then be fitted to equations (4) and (5) using the values of  $\tau$  and  $\omega_0$  determined above, to give  $\hbar\omega_p = 11.4 \pm 0.2$  eV (figure 7).

There are clear systematic discrepancies between the theoretical fits and the experimental data shown in figure 7. It should be noted that even though the reflectivity measurements were carried out over a very limited frequency range, the general trends in the model are clear in the experimentally determined results.

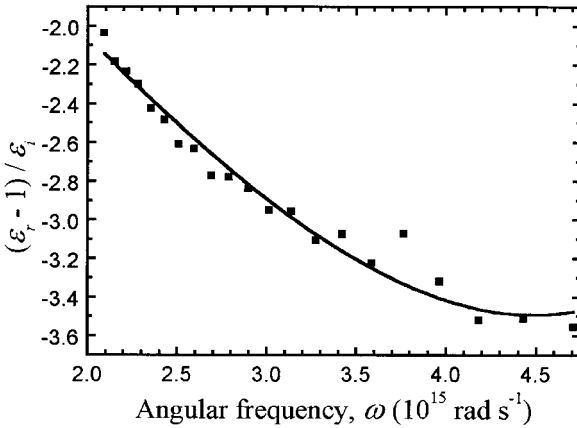


Figure 6. By assuming a one-resonance Drude–Lorentz model, a function relating the real and imaginary parts of the dielectric function may be obtained (equation (6)). By fitting this function to the experimental data, values of  $\tau$  and  $\omega_0$  are obtained.

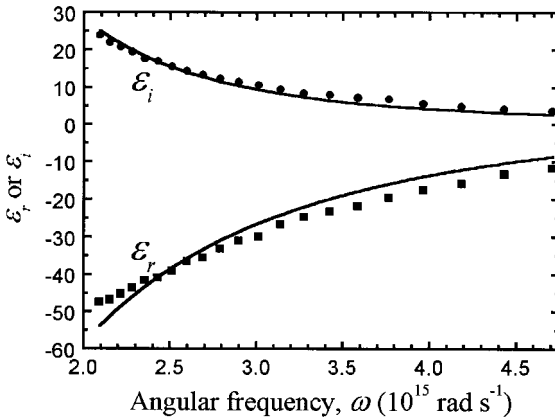


Figure 7. The results of fitting equations (4) and (5) to the complex dielectric function of indium determined in this study. The solid lines represent the theoretical fits, and the squares and circles represent the experimentally determined values of  $\epsilon_r$  and  $\epsilon_i$  respectively. Hence, the Drude–Lorentz model may be used as an approximation to obtain a value of  $\omega_p$ .

Furthermore, the two values of  $\hbar\omega_p$  determined by fitting the real and imaginary parts of the dielectric function individually differ only by 0.1 eV. The discrepancy at low frequencies, particularly in the  $\epsilon_r$  data, may be due to the effect of a second absorption band. In fact, an interband transition in the region of  $2.0 \times 10^{15} \text{ rad s}^{-1}$  (1.3 eV) has been experimentally observed [13], and would agree with the results presented here.

However, it is clear, that neither the simple Drude mode, nor the one-resonance Drude–Lorentz model describe indium accurately over the frequency range studied. A more sophisticated mode is therefore required, but such a multiple-resonance model would have many degenerate solutions to the limited range of experimental data presented here.

## 5. Conclusions

The complex dielectric function of non-oxidized indium has been experimentally determined throughout the visible regime using a grating-coupled SPP technique. This has been achieved by fitting the reflectivity measurements from a metal–dielectric interface to the predictions from a rigorous grating-modelling theory, using the grating profile and the complex dielectric constants of indium as fitting parameters. A comparison of the constants determined from this work, with those from a previous study suggests a strong dependence of the dielectric function on the film thickness and deposition conditions.

The plasma frequency and relaxation time have been calculated by fitting the measured dielectric function to a simple Drude model. However, the free-electron model has been demonstrated to be inadequate, and a more sophisticated one-resonance model has also been used. Systematic discrepancies between the modelled and measured dielectric functions illustrate that this model is also somewhat too simplistic. However, the values of the relaxation time determined from both models are consistent, and the values of the plasma frequency obtained by fitting the second model to both  $\epsilon_r$  and  $\epsilon_i$  show excellent agreement.

## Acknowledgments

The authors wish to thank The Royal Society, DERA (Farnborough) and the EPSRC for the financially supporting this study.

## References

- [1] KRETSCHMANN, E., and RAETHER, H., 1968, *Z. Naturforsch. A*, **23**, 2135.
- [2] OTTO, A., 1968, *Z. Phys.*, **216**, 398.
- [3] SCHRÖDER, U., 1981, *Surf. Sci.*, **102**, 118.
- [4] POCKRAND, I., 1974, *Phys. Lett.*, **49A**, 259.
- [5] NASH, D. J., and SAMBLES, J. R., 1996, *J. mod. Optics*, **43**, 81.
- [6] RITCHIE, R. H., ARAKAWA, E. T., COWAN, J. J., and HAMM, R. N., 1968, *Phys. Rev. Lett.*, **21**, 1530.
- [7] NASH, D. J., COTTER, N. P. K., WOOD, E. L., BRADBERRY, G. W., and SAMBLES, J. R., 1995, *J. mod. Optics*, **42**, 243.
- [8] INNES, R. A., and SAMBLES, J. R., 1987, *J. Phys. F: Metal Phys.*, **17**, 277.
- [9] TILLIN, M. D., and SAMBLES, J. R., 1988, *Thin Solid Films*, **167**, 73.
- [10] TILLIN, M. D., and SAMBLES, J. R., 1989, *Thin Solid Films*, **172**, 27.
- [11] NASH, D. J., and SAMBLES, J. R., 1998, *J. mod. Optics*, **45**, 2585.
- [12] NASH, D. J., and SAMBLES, J. R., 1995, *J. mod. Optics*, **42**, 1039.
- [13] THEYE, M. L., and DEVANT, G., 1969, *Thin Solid Films*, **4**, 205.
- [14] KOVACS, G. J., 1979, *Thin Solid Films*, **60**, 33.
- [15] AGEEV, L. A., and SHKLYAREVSKII, I. N., 1968, *Sov. Phys. Solid State*, **9**, 2324.
- [16] GOLVASHKIM, A. I., LEVCHENKO, I. S., MOTULEVICH, G. P., and SHUBIN, A. A., 1967, *Sov. Phys. JETP*, **24**, 1093.
- [17] BURTIN, R., 1964, *Rev. Optics*, **43**, 463 and 618.
- [18] EL OKER, M. M., ABOU-SAIF, E. A., EL SAHAR, S. A., and MOHAMED, A. A., 1982, *Phys. status solidi a*, **73**, 389.
- [19] COTTER, N. P. K., PREIST, T. W., and SAMBLES, J. R., 1995, *J. opt. Soc. Am.*, **12**, 1097.
- [20] CHANDEZON, J., DUPUIS, M. T., CORNET, G., and MAYSTRE, D., 1982, *J. opt. Soc. Am.*, **72**, 839.